Available online at www.sciencedirect.com
SCIENCE DIRECT®
Journal of Organometallic Chemistry 691 (2006) 1984–1992
Journal of Organometallic Chemistry
www.elsevier.com/locate/jorganchem

An experimental–theoretical approach to the kinetics and mechanism of Michael type addition: α,β-Unsaturated tungsten Fischer carbene complex as the substrate

Kaichun Gu [a], Gang Yang [a], Weiping Zhang [a], Xiumei Liu [a], Zhengkun Yu [b], Xiuwen Han [a,*], Xinhe Bao [a]

[a] State Key Laboratory of Catalysis, Dalian Institute of Chemical Physics, Chinese Academy of Sciences, 457 Zhongshan Road, Dalian, Liaoning 116023, PR China

[b] Dalian Institute of Chemical Physics, Chinese Academy of Sciences, 457 Zhongshan Road, Dalian, Liaoning 116023, PR China

Received 14 November 2005; received in revised form 23 December 2005; accepted 27 December 2005
Available online 21 February 2006

Abstract

Through variable-temperature ^{1}H and ^{13}C NMR experiments and density functional calculations, the kinetics and mechanism of Michael type addition were investigated using alkynyl carbene **A** as the substrate. The two conformers of substrate **A** were distinguished from the ^{1}H and ^{13}C NMR spectra, and the calculated results showed that the *syn*-conformer is more stable than the *anti*- by 6.5 kJ mol^{-1} with the activation barrier between these two conformers as 62.5 kJ mol^{-1}. The full reaction mechanism of Michael type addition was first presented to us, which differs from the previous solely based on the kinetic studies. It contains three elementary steps (see the scheme): (1) Formation of C_8–N_2 bond via transition state $\mathbf{TS}_1$. (2) Conformation conversion from $\mathbf{In}_1$ to $\mathbf{In}_2$, which is very important but ignored before. (3) Intramolecular proton transfer via transition state $\mathbf{TS}_2$ forming the product. The first step is rate determining with an activation barrier of 73.0 kJ mol^{-1}, very close to the experimental value of 89.6 kJ mol^{-1}. The product **P** is dominant over **P′** in population contrary to the situation of tautomer **B′** over **B**, which is caused by larger activation barriers to **P′** and the less stabilities of structures related to **B′** from the first transition state to the product.

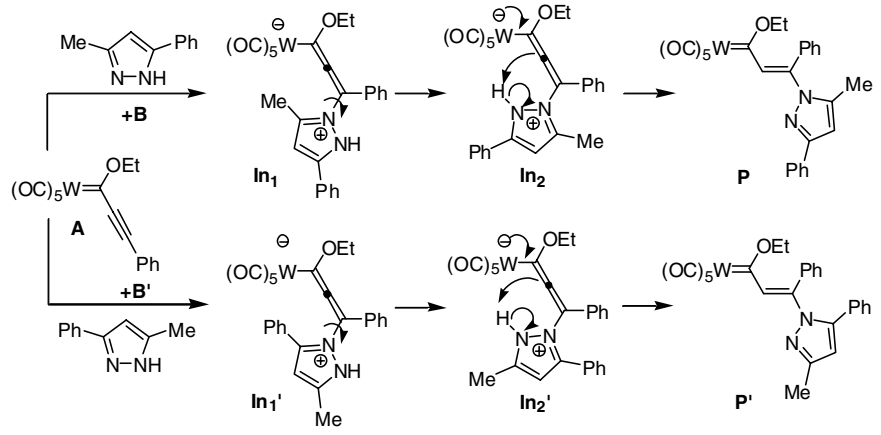

* Corresponding author.
E-mail address: xwhan@dicp.ac.cn (X. Han).

0022-328X/$ - see front matter © 2006 Elsevier B.V. All rights reserved.
doi:10.1016/j.jorganchem.2005.12.063

Keywords: α,β-Unsaturated Fischer carbene complexes; Michael type addition; NMR; Density functional calculations; Activation barrier

1. Introduction

In the past two decades, the chemistry of Fisher carbene complexes, especially the α,β-unsaturated [1], has attracted increasing attention from various synthetic groups [2]. They are involved in the formation of phenol (Dötz product) [3] and indene derivatives [4]. They also act as the intermediates to pyridines [5], pyrroles [6], cyclopentenones [7], cyclopenta-[*b*]pyrans [8] and other heterocyclic complexes [9].

To the diverse reactions mediated with these Fischer carbene complexes, the mechanistic studies lag far behind the synthetic aspects [10]. Much progress has been made on the mechanisms for the hydrolysis of alkyl or aryl carbene complexes [11], the photocarbonylation of chromium carbene complex [12] as well as the Dötz reaction [13]. However, the mechanism of Michael type addition, a more general reaction, is still far from clarity. Based on the activation parameters using the pyrrolidine as the nucleophile, van Eldik et al. [14] followed a two-step mechanism with a zwitterionic intermediate involved, which was much more polar than the reactants. A small solvent dependence was observed probably due to the charge delocalization over the $M(CO)_5$ fragment (M = Cr, Mo or W) [15,16]. Large negative reaction constant ($\upsilon = -2.95$) suggested the sensitivity of Michael type addition against the electronic effects [17]. The zwitterionic intermediate was unstable to detect experimentally. Moreover, the mechanism proposed above was solely based on the kinetic studies, which lacks direct proof and needs further investigation.

Recently, a series of β-pyrazolato-α,β-unsaturated tungsten Fisher carbenes have been successfully produced in our group, see Scheme 1 [18]. To investigate the kinetics and mechanism of Michael type addition, the manuscript was organized as below: (1) Substrate **A**, which has different conformers, was subject to variable-temperature ^1H and ^{13}C NMR experiments. The interconversion process between the conformers of substrate **A** should be well understood before the investigation of Michael type addition. (2) The kinetics of Michael type addition was monitored under in situ ^1H NMR technique and then the activation parameters were obtained. (3) The transition state was located for the conformers of substrate **A** by density functional calculations. (4) Mechanism of Michael type addition was proposed after geometrically optimizing a series structures and transition state searching. (5) The problem why the dominant tautomer **B′** will result in the minor product **P** was tackled.

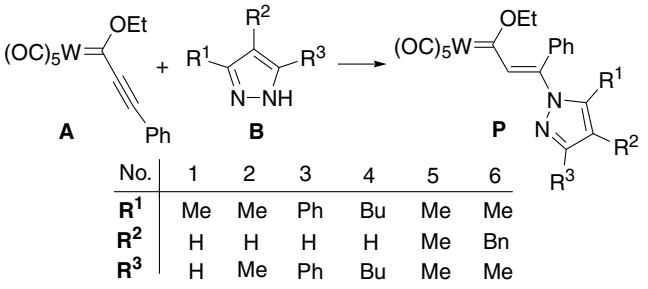

No.	1	2	3	4	5	6
R1	Me	Me	Ph	Bu	Me	Me
R2	H	H	H	H	Me	Bn
R3	H	Me	Ph	Bu	Me	Me

Scheme 1. Synthesis of β-pyrazolato-α,β-unsaturated carbenes.

2. Experimental

The alkynyl Fischer tungsten carbene complex **A** and 3-methyl-5-phenylpyrazole **B** were prepared and purified as described elsewhere [19,20]. The samples were dissolved in $CDCl_3$ for the NMR measurements, with the initial concentrations of **A** and **B** both as 0.04 mol L^{-1}. All the NMR spectra were recorded on Bruker DRX-400 NMR spectrometer equipped with a 5 mm indirect detection probe with Z-gradient (chemical shifts were referred to TMS). To carry out the kinetic investigation, the ^1H NMR spectra were acquired with time interval of 10 min. Net ethylene glycol was used as the thermometer substance calibrating the NMR measurement temperatures [21].

3. Calculation details

Density-functional calculations were performed at the gradient corrected approximation level, implemented in the DMOL3 program, CERIUS 2 of MSI [22]. Joubert and Maldivi [23] claimed that BP functional was superior to the conventional B3LYP functional when treating systems with heavy elements, confirmed by our pervious theoretical work [24]. Accordingly, BP functional was employed here along with the high precise basis set of DNP. All the elements were calculated with all electrons except W, whose core electrons were replaced by a simple effective core potential (ECP) with the valence electrons treated as 5s5p5d6s6p.

To describe the mechanism of Michael type addition as accurate as possible, the most precise transition state searching method in DMOL3 module was selected; i.e., complete linear synchronous transit/quadratic synchronous transit (complete LST/QST) protocol.

4. Results and discussion

4.1. The features of ^1H and ^{13}C NMR spectra

4.1.1. Interconversion between the conformers of substrate *A*

From the variable temperature ^1H NMR spectra in Fig. 1, it was found that at the temperature range of −60 to −20 °C, the proton signals for methylene or methyl of ethoxyl (CH_3CH_2O) are separated into two groups, corresponding to the *syn*- and *trans*-conformer, respectively.

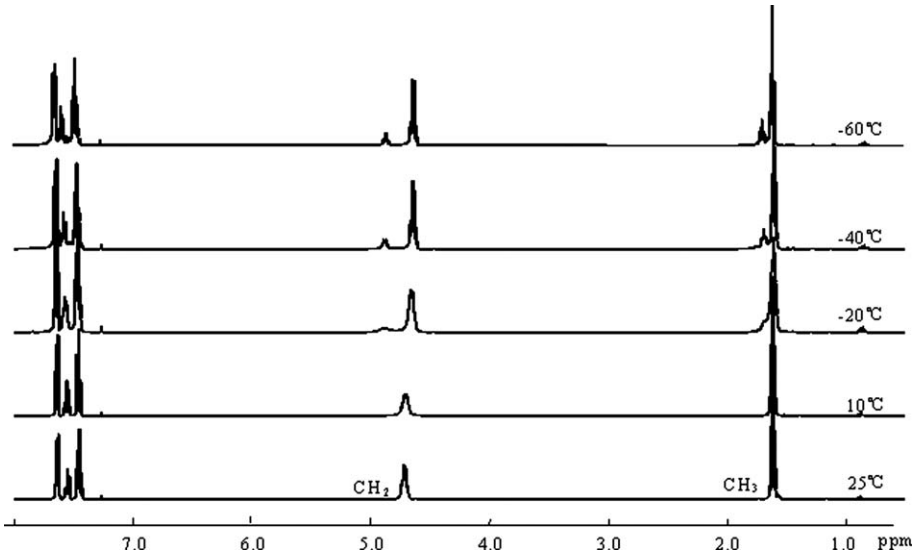

Fig. 1. Variable temperature ^{1}H NMR spectra of substrate **A**.

At −60 °C, the ratio of main/minor conformers is 4.6 based on the ^{1}H NMR integrals. Variable temperature ^{13}C NMR spectra also evidence the coexistence of two conformers: 284.9 and 289.8 ppm for carbene carbon in the main and minor conformers, 206.6 and 205.3 ppm for *trans*-CO, 197.7 and 196.9 ppm for *cis*-CO, 133.4, 132.1, 129.0, 120.1 and 132.9, 132.2, 128.9, 122.0 ppm for phenyl carbons, 131.5 and 122.0 ppm for ≡C(–Ph), 96.5 and 100.0 ppm for C(≡C–Ph), 75.8 and 79.2 ppm for CH_2, 14.7 and 15.0 ppm for CH_3, respectively, see Fig. 2. The resonance of carbene carbon in the minor conformer is at lower field than that in the main one, which implies that the former is of more electron deficiency. The main conformer of alkynyl-substituted carbene complex **A** will adopt *syn*-configuration [25], confirmed by our latter calculated results with the *syn*-conformer stabilized by 6.5 kJ mol^{-1} over the *anti*. At low temperatures, the interconversion process is quite slow, where the two conformers can be distinguished from ^{1}H and ^{13}C NMR spectra. As the temperature increases, ^{1}H and ^{13}C NMR signals become broadened and coalesced and finally turn out sharp, where the interconversion process proceeds fast on the NMR time scale.

4.1.2. Michael type addition

As Scheme 2 shows, 3-methyl-5-phenylpyrazole (**B**) and 3-phenyl-5-methylpyrazole (**B′**) are two tautomers, with **B′** of higher proportion [26]. The Michael type addition of **B** and **B′** leads to two products; i.e., **P** through reaction 1 and **P′** through reaction 2, respectively.

The characterization of the products was performed by in situ ^{1}H NMR spectroscopy, see Fig. S1, with the chemical shifts collected in Table 1. Compared to **B** or **B′**, the ^{1}H NMR signals of methyl in the products shift upfield due to the

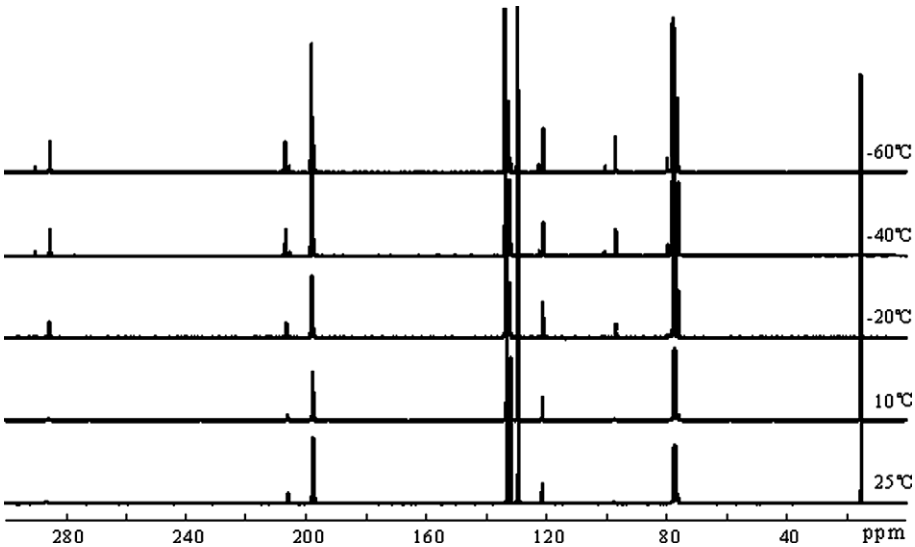

Fig. 2. Variable temperature ^{13}C NMR spectra of substrate **A**.

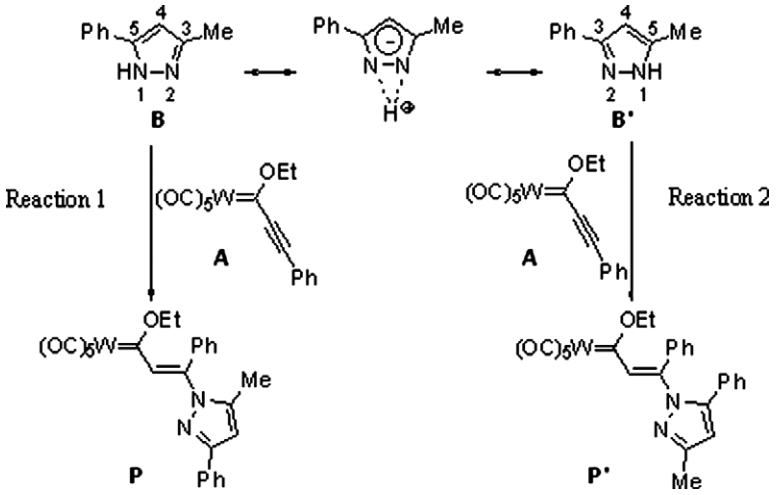

Scheme 2. Tautomers for the substituted pyrazole and their products.

Table 1
^{1}H NMR chemical shifts for Michael type addition (units in ppm)

	OCH_2	$(OCH_2)CH_3$	4-H(pyrazole)	CH_3(pyrazole)
A	4.72 and 4.70	1.58	–	–
B (**B**′)	–		6.35	2.38
P	4.56 and 4.52	0.98	6.45	1.82
P′	4.47 and 4.44	0.91	6.23	2.37

electron donation by *N*-alkenylation of pyrazole [27]. The anisotropic shielding effect as another important factor exists in the phenyl ring of **P**, which results in the up-field shifts of methyl in **P** (about 224 Hz) more obviously than in **P**′ (about 4 Hz) [28]. It was observed from our ^{1}H NMR spectra that the minor tautomer **B** will lead to the main product **P** whereas the main tautomer **B**′ to the minor product **P**′, and the reasons will be elaborated in Section 4.5.

4.2. Reaction rates and activation parameters based on NMR experiments

From the ^{1}H NMR spectra of Michael type at different reaction times (Fig. 3), it can be seen that the concentrations of reactants and products will change as the reaction proceeds, reflected by the intensities of the corresponding peaks. The peaks at 4.72 and 4.70 ppm are assigned to the methylene protons of substrate **A** whereas at 4.56, 4.52 and 4.47, 4.44 ppm to the methylene protons of products **P** and **P**′, respectively. The concentration of substrate **A** and its reciprocal were plotted against the reaction time (see Fig. 4). The inverse concentration can be expressed through the following equation

$$1/[\mathbf{A}] = kt + \text{Constant} \quad (1)$$

where [**A**] represents the concentration of substrate **A** and k the overall rate constant. Obviously, the reaction is second order, namely a bimolecular reaction. At each specified temperature, the ratio of [**P**′]/[**P**] (labelled as θ) remains almost invariable within two half-lives, implying that reactions 1 and 2 proceed under the same mechanism. Accordingly, the rate constants of reactions 1 and 2; i.e., k_1 and k_2 can be obtained by the equations below

$$k_1 = k/(1+\theta) \quad (2)$$

$$k_2 = k\theta/(1+\theta) \quad (3)$$

The temperature dependences of k_1 and k_2 are summarized in Table 2. Within the Eyring transition state theory, the

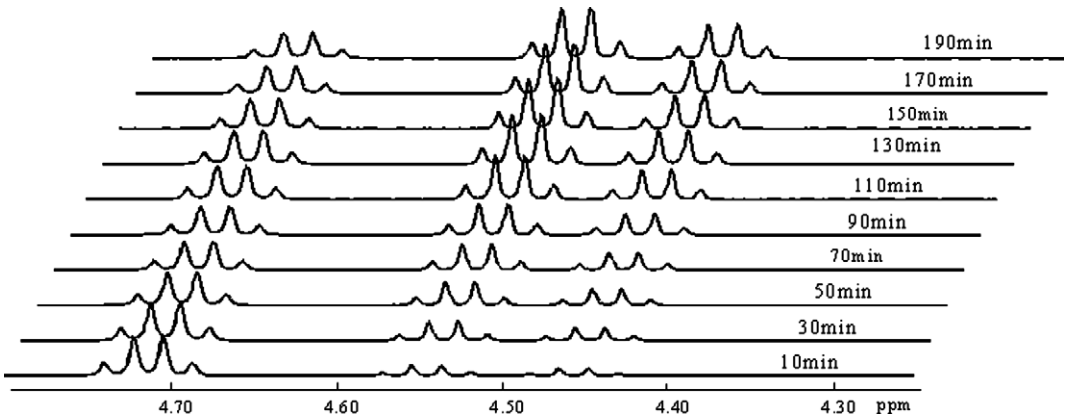

Fig. 3. ^{1}H NMR spectra for Michael type reaction at different times.

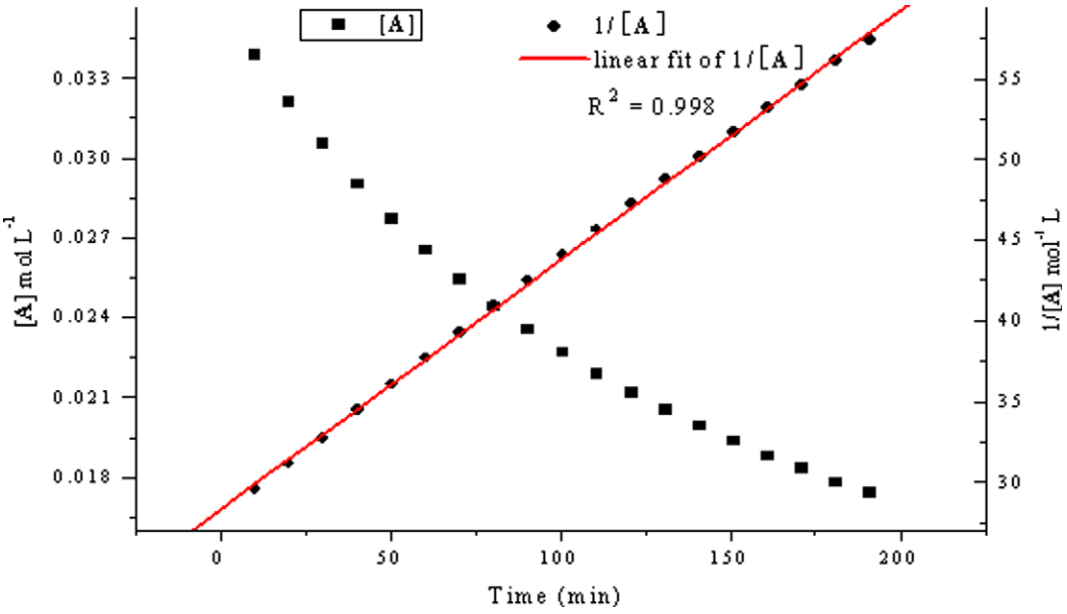

Fig. 4. Plots of the concentration of substrate **A** and its reciprocal vs. the reaction time.

Table 2
Rate constants and activation parameters of Michael type addition in solvent $CDCl_3$

	Temperature (°C)	k_1 or k_2 (10^3 M^{-1} s^{-1})	k (25 °C) (10^3 M^{-1} s^{-1})	$\Delta H^{\ddagger}$ (kJ mol^{-1})	$\Delta S^{\ddagger}$ (J mol^{-1} K^{-1})	$\Delta G^{\ddagger}$ (25 °C) (kJ mol^{-1})
Reaction 1	35	1.4	0.7	58.4	−109.6	91.1
	40	2.4				
	45	3.4				
	50	4.4				
Reaction 2	35	1.0	0.5	52.6	−131.0	91.7
	40	1.6				
	45	2.2				
	50	2.9				

corresponding activation parameters were obtained and listed in Table 2. The Michael type addition reaction is characterized by low activation enthalpy ($\Delta H^{\ddagger} = 58.4$ and 52.6 kJ mol^{-1}) and large activation entropy ($\Delta S^{\ddagger} = -109.6$ and -131.0 J mol^{-1} K^{-1}), consistent with the results of van Eldik et al. [15,16]. k_2/k_1 decreases as 0.73 at 35 °C > 0.69 at 40 °C > 0.66 at 45 °C ≈ 0.66 at 50 °C, which indicates that reaction 1 is more favored over reaction 2 as the temperature goes up.

4.3. Theoretical investigation on the syn/anti interconversion of substrate A

At low temperatures, there exist two different conformers for substrate **A**, as observed in our ^1H and ^{13}C NMR experiments. For the two conformers, the calculated C–O distances of all the five carbonyls fall at ca. 1.60 Å, and all the W–C bond lengths are approximately at 2.08 Å except the one associated with the carbene carbon which falls at about 2.19 Å. The validity of our theoretical methods have been depicted in Section 3, which is further verified by optimizing $(CO)_5W{=}C(OEt){-}C{=}C(R^1R^2R^3pz)Ph$ ($R^1 = R^3 =$ *t*-Bu, $R^2 = H$, see Fig. S2) and then comparing the calculated geometric parameters with those from X-ray diffraction experiments, see the details in Table S1. As shown in Fig. 5, the *syn*-conformer is more stable than the *anti* by 6.5 kJ mol^{-1}. In the *syn*-conformer, the ethoxyl group falls almost within the C_2–C_3–C_5–W–C_6 plane, which can be deduced from the small C_5–W–C_6–O_6 dihedral angle of −4.2°, whereas the ethoxyl group in the *anti*-conformer deviates greatly from the C_2–C_3–C_5–W–C_6 plane with the C_5–W–C_6–O_6 dihedral angle of 45.0°. Accordingly, the electronic donation from ethoxyl to the p_z orbitals of carbene atoms will be more facilitated in the *syn*-conformer and thus stabilizes this conformer [29].

The activation barrier for this interconversion process is calculated at 62.5 kJ mol^{-1}, close to the value 59.8 kJ mol^{-1} for an alkyl chromium Fisher carbene. The dihedral angle of W–C_6–O_6–C_{10} changes from −1.0° in the *syn*-conformer to 78.7° in the transition state **TS** and then to −179.3° in the *anti*-conformer. Compared to the two conformers, the W–C_6 and C_6–C_7 bonds in **TS** are strengthened somewhat at the expense of weakening C_6–O_6 bond (see the exact values in Fig. 5). The remaining part of the α,β-unsaturated Fisher carbene seems unaffected during the interconversion process.

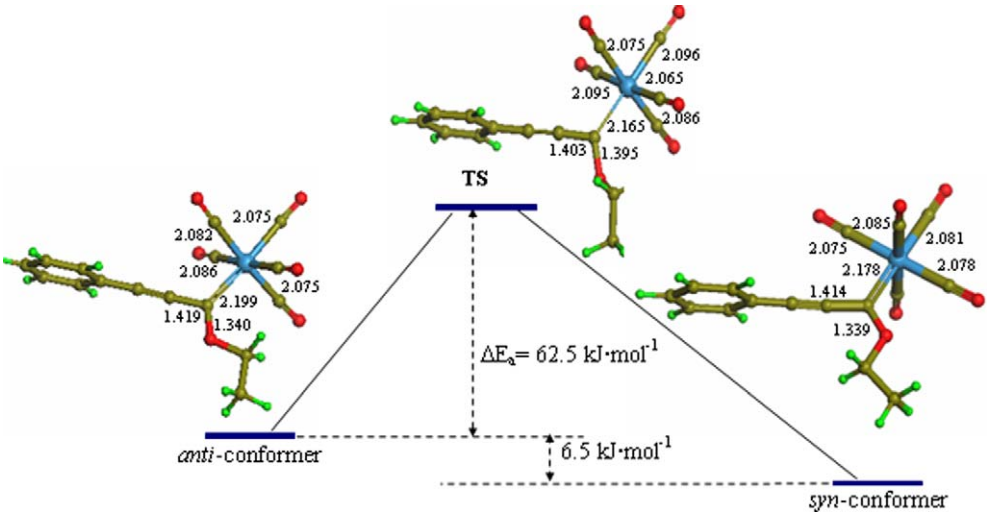

Fig. 5. *Anti/syn* interconversion for α,β-unsaturated tungsten Fischer carbene **A**.

4.4. Theoretical investigation on the reaction mechanism of Michael type addition

4.4.1. Structures of reactants, intermediates and products

The adsorption structure of 3-methyl-5-phenylpyrazole **B** on α,β-unsaturated Fisher carbene **A** is marked as **A** − **B**, and the two intermediates as $\mathbf{In}_1$ and $\mathbf{In}_2$, respectively (see Fig. 6).

For substrate **A**, the calculated data show that the *syn*-conformer is slightly more stable than *anti*-conformer. Our X-ray diffraction and NMR experiments suggest the products adopt predominantly the *anti*-conformer. Accordingly, the interconversion between the two conformers of substrate **A** will take place due to the small activation barrier, and the mechanism of Michael type addition can be elucidated on the *anti*-conformers.

In structure **A** − **B**, the C_8–N_2 distance is optimized at a large value 4.308 Å. The geometries of **B** and **A** seem unaffected (see Table 3), which implies a weak adsorption with energy of 9.9 kJ mol^{-1}. C_7–C_8 is characteristic of triple bond with the length of 1.230 Å.

The formation of $\mathbf{In}_1$ destroys the triple C_7–C_8 bond in substrate **A** with the length elongated to 1.329 Å. Meanwhile, the overlap of π electrons between the phenyl and alkynyl (C_7–C_8) groups is significantly decreased, as concluded from the variation of the C_7–C_8–C_9 angle (179.4–129.1°). Therefore, the stability of structure $\mathbf{In}_1$ is reduced compared to structure **A** − **B**, supported with the result that $\mathbf{In}_1$ is higher in energy than **A** − **B**.

$\mathbf{In}_2$ is in equilibrium with to $\mathbf{In}_1$. Their structures are very close to each other, which can be deduced from the geometric parameters (Table 3). The largest difference between

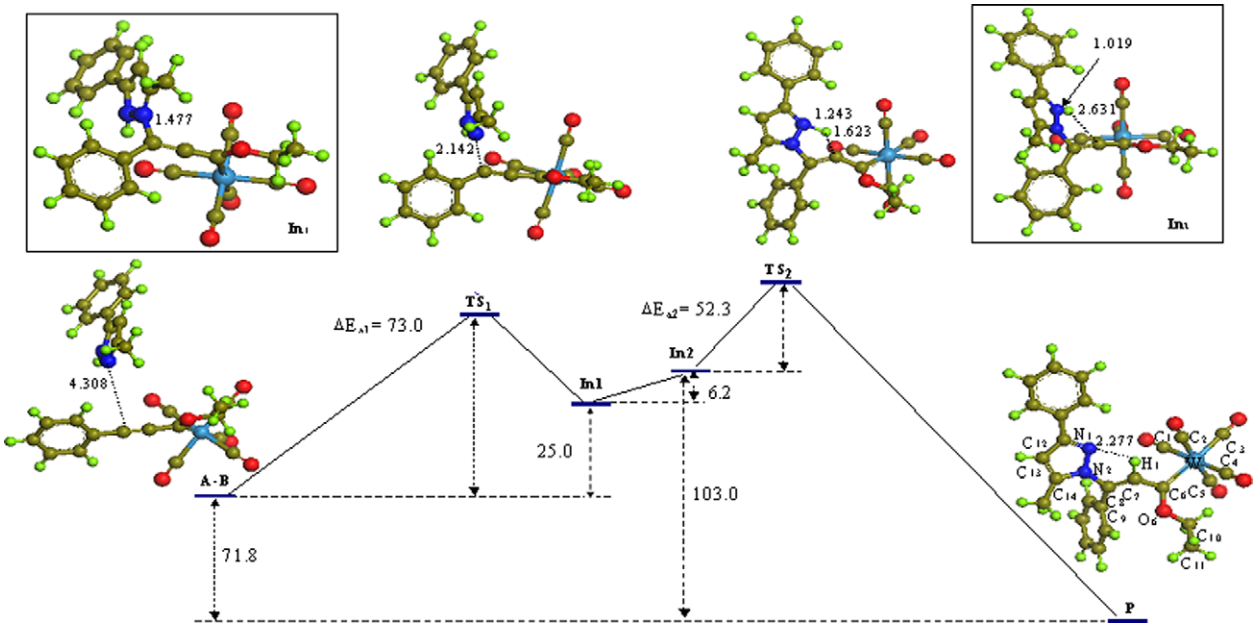

Fig. 6. Reaction mechanism of Michael type addition from theoretical calculations (energy units in kJ mol^{-1}).

Table 3
Geometric parameters of reactants, intermediates, products as well as the transition states of Michael type addition (bond lengths in Å and angles in °)

	A + B	**A − B**	**TS_1**	**In_1**	**In_2**	**TS_2**	**P**	**A + B′**	**A − B′**	**TS'_1**	**In'_1**	**In'_2**	**TS'_2**	**P′**
W–C_6	2.199	2.212	2.293	2.347	2.350	2.275	2.239	2.199	2.214	2.304	2.350	2.341	2.275	2.232
C_6–C_7	1.419	1.411	1.373	1.322	1.325	1.395	1.456	1.419	1.411	1.374	1.322	1.323	1.389	1.457
C_7–C_8	1.229	1.230	1.260	1.329	1.331	1.353	1.368	1.229	1.230	1.257	1.328	1.329	1.347	1.369
C_8–C_9	1.421	1.416	1.432	1.476	1.480	1.481	1.487	1.421	1.416	1.443	1.476	1.478	1.486	1.485
C_6–O_6	1.340	1.341	1.349	1.377	1.373	1.361	1.332	1.340	1.339	1.349	1.374	1.376	1.361	1.333
N_1–N_2	1.353	1.353	1.349	1.368	1.359	1.346	1.371	1.350	1.351	1.351	1.369	1.477	1.470	1.374
N_1–C_{14}	1.369	1.368	1.368	1.358	1.358	1.374	1.336	1.367	1.365	1.362	1.353	1.354	1.370	1.334
C_8–N_2		4.308	2.142	1.477	1.467	1.462	1.423		4.333	2.029	1.481	1.477	1.470	1.427
N_1–H_1				1.026	1.019	1.243	2.277				1.026	1.022	1.245	2.341
C_7–H_1				3.282	2.631	1.623	1.088				3.242	2.573	1.604	1.088
W–C_6–C_7	118.5	118.0	114.5	111.4	111.4	112.9	117.9	118.5	117.8	113.9	111.5	111.9	113.0	118.6
O_6–C_6–C_7	107.8	108.4	110.9	116.0	116.2	113.9	110.4	107.8	108.4	112.0	116.5	115.9	113.6	110.3
C_6–C_7–C_8	177.8	178.0	175.8	174.5	167.9	138.3	130.1	177.8	177.8	175.1	174.7	175.3	141.9	129.7
C_6–C_7–H_1					112.9	132.3	114.9					107.4	128.2	114.9
C_7–C_8–C_9	176.2	179.4	143.3	129.1	127.1	133.4	126.7	176.2	179.3	140.8	129.0	128.1	134.7	127.8
C_7–C_8–N_2		93.4	109.8	116.0	117.2	112.1	117.2		93.8	111.8	116.4	115.6	110.6	119.4
C_5–W–C_6–O_6	45.0	47.9	13.3	2.8	0.3	−22.6	36.9	45.0	48.4	10.1	1.0	−0.5	−22.0	35.0

them is the direction of H_1 atom (see Fig. 6), which leads to the distance between H_1 and C_7 changing from 3.282 in **In_1** to 2.631 Å in **In_2** and the angle of C_7–C_8–H_1 changing from 108.3° in **In_1** to 77.2° in **In_2**.

To the product **P**, C_6, H_1, C_7, C_8, C_9 and N_2 are almost within the same plane, and the C7–C8 is of double bond with the length of 1.368 Å. The part of $W(CO)_5COEt$ restores greatly to the original state as in substrate **A**.

As to C–O bonds in the carbonyls, they remain almost constant during Michael type addition. Except the W–C_6 bond, the other five W–C bonds are also uninfluenced.

4.4.2. Reaction mechanism of Michael type addition

The reaction mechanism of Michael type addition was proposed and displayed in Fig. 6. Here the two transition states are located and marked as **TS_1** and **TS_2**, respectively. The reaction contains three steps:

(1) Formation of C_8–N_2 bond leading to the first intermediate **In_1**. The N_1 atom is excluded from the nucleophilic center [30]. This step is endothermic with reaction heat as 25.0 kJ mol^{-1}. The activation barrier is calculated to be 73.0 kJ mol^{-1}.
(2) Conformation conversion from **In_1** to **In_2** through the rotation of C_8–N_2 bond. The slight energy difference (6.2 kJ mol^{-1}) between them means these two conformations are in fast equilibrium. However, the conversion is absolutely essential, for the reorientation of H_1 atom ensures step 3 to take place.
(3) Intramolecular proton transfer forming the product **P**. This step is largely exothermic with reaction heat of −103.0 kJ mol^{-1}. The activation barrier is calculated at 52.3 kJ mol^{-1}. IRC was computed from **In_2** to **TS_2**, with the C_7–H_1 bond length at 2.600, 2.300, 2.000, 1.900, 1.800 or 1.700 Å, respectively. Along the reaction pathway, the energy is monotonous ascending until reaching **TS_2**. Meanwhile, the structures gradually change away from **In_2** towards **TS_2**. Accordingly, it is the intermediate **In_2** that climbs over the transition state **TS_2** and reaches the final product **P**.

To conclude, the Michael type addition (from step 1 to step 3) is exothermic with the calculated reaction heat as −81.7 kJ mol^{-1}. As the activation barrier of the first step is larger than that of the third step and the former is endothermic whereas the latter exothermic, it should be the first step as rate determining. The activation barrier of the first step is close to the experimental activation enthalpy of 89.6 kJ mol^{-1}. van Eldik et al. [14] used secondary amines as the nucleophiles to study the kinetics and also obtained that the first step is rate determining. A more systematic analysis of Michael type addition will be carried out in future work with different R^1, R^2 and R^3 in pyrazole considered.

The Mulliken charges on pyrazolyl, $W(CO)_5$ and fragment 1 (including $W(CO)_5$, OEt, C_6, C_7 and C_8) increase from **A + B** to the intermediates (**In_1**, **In_2**), and then decrease until the formation of the final product **P** (see Fig. 7). The first transition state (**TS_1**) is more polar than the reactant (**A + B** or **A − B**), and the second (**TS_2**) than the product **P**. Intermediates **In_1** and **In_2** are zwitterionic intermediates with the largest charge separation. It is considered that the negative charge center should be more precisely as $W(CO)_5$ instead of the larger fragment 1 by van Eldik et al. [14].

4.5. Theoretical investigation on the reason why *P* is dominant over *P′*

Two products **P** and **P′** appear due to the coexistence of tautomers **B** and **B′** (see Scheme 2). Parallel theoretical calculations were performed on tautomer **B′** reacting with substrate **A**. "′" is added to all the structures related to tautomer **B′**. The activation barrier for the first step is calculated at 80.1 kJ mol^{-1}, and for the third step at 55.6 kJ mol^{-1}. Both are larger than those related to the tautomer **B**, which may lead to the more population of **P** over **P′**.

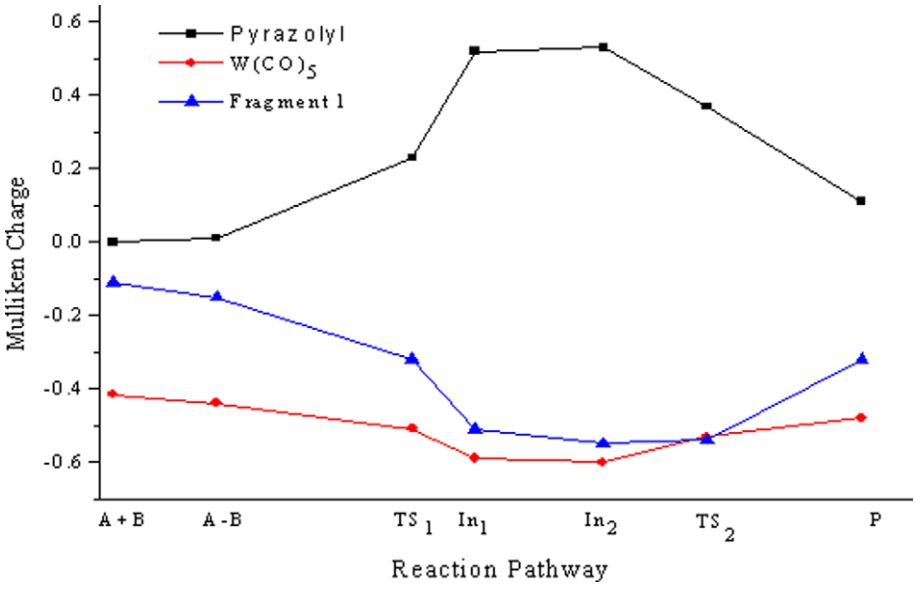

Fig. 7. Changes of Mulliken charges along the reaction pathway.

Table 4
Energy differences between the structures related to **B** and **B′**

$\Delta E_{\mathbf{B}}$ (kJ mol^{-1})	$\Delta E_{\mathbf{A-B}}$ (kJ mol^{-1})	$\Delta E_{\mathbf{TS_1}}$ (kJ mol^{-1})	$\Delta E_{\mathbf{In_1}}$ (kJ mol^{-1})	$\Delta E_{\mathbf{In_2}}$ (kJ mol^{-1})	$\Delta E_{\mathbf{TS_2}}$ (kJ mol^{-1})	$\Delta E_{\mathbf{P}}$
1.2	1.7	−5.4	−9.9	−6.6	−9.8	−11.6

The energy difference between the tautomers **B** and **B′** is defined as $\Delta E_{\mathbf{B}}$, and $\Delta E_{\mathbf{A-B}}$, $\Delta E_{\mathbf{TS1}}$, $\Delta E_{\mathbf{In_1}}$, $\Delta E_{\mathbf{In_2}}$, $\Delta E_{\mathbf{TS2}}$ and $\Delta E_{\mathbf{P}}$ for energy differences between the structures related to **B** and **B′**, respectively (see the exact values in Table 4). As expected, **B** is less stable than **B′** with a calculated energy difference of 1.2 kJ mol^{-1}. The stabilities of the absorbed structures are the same in sequence. However, the situation changes from the first transition state, where $\mathbf{TS_1}$ is found more stable than $\mathbf{TS'_1}$ by 5.4 kJ mol^{-1}. The largest energy difference is for the two products, where **P** is favored over **P′** by 11.6 kJ mol^{-1}. For structures related to **B′**, the energy differences are reverse in sequence to the distances between the two phenyls, suggesting that it be the repulsion between these two bulk phenyls that reduces their stabilities.

5. Conclusions

1. By variable-temperature ^{1}H and ^{13}C NMR experiments, the *syn*- and *anti*-conformers of substrate **A** were distinguished. The calculated results showed that the *syn*-conformer is more stable than the *anti*- by 6.5 kJ mol^{-1}, and that the activation barrier between these two conformers is 62.5 kJ mol^{-1}.
2. From kinetic analysis based on the ^{1}H NMR experiments, Michael type addition is of second order, characterized by low activation enthalpy and significantly negative activation entropy.
3. The reaction mechanism of Michael type was proposed, which contains three elementary steps crossing over two intermediates and two transition states. Intermediates $\mathbf{In_1}$ and $\mathbf{In_2}$ are zwitterionic intermediates with the largest charge separation.
4. According to the calculated results, the first step is rate determining. The activation barrier of this step is calculated as 73.0 kJ mol^{-1}, very close to the experimental value of 89.6 kJ mol^{-1}.
5. The more population of product **P** over **P′** is caused by two reactions: (i) The smaller activation barrier of tautomer **B** than **B′** when reacting with substrate A. (ii) The less stabilities of the structures related to **B′** from the first transition states.

Acknowledgements

We gratefully acknowledge the financial support from the Foundation of China Ministry of Science and Technology of China (National Key Project of Fundamental Research: No. 2003CB615806).

Appendix A. Supplementary data

Supplementary data associated with this article can be found, in the online version, at doi:10.1016/j.jorganchem.2005.12.063.

References

[1] A. de Meijere, H. Schirmer, M. Duetsch, Angew. Chem., Int. Ed. Engl. 39 (2000) 3964.

[2] (a) R. Aumann, H. Nienaber, Adv. Organomet. Chem. 41 (1997) 163;
(b) W.D. Wulff, Organometallics 17 (1998) 3116;
(c) K.H. Dötz, P. Tomuschat, Chem. Soc. Rev. 28 (1999) 187;
(d) J.W. Herndon, Coordin. Chem. Rev. 206 (2000) 237;
(e) M.A. Sierra, Chem. Rev. 100 (2000) 3591;
(f) J. Barluenga, J. Santamaria, M. Tomas, Chem. Rev. 104 (2004) 2259.

[3] (a) K.H. Dötz, Angew. Chem. 87 (1975) 672;
Angew. Chem., Int. Ed. Engl. 14 (1975) 644;
(b) K.H. Dötz, R. Dietz, A. von Imhof, H. Lorenz, G. Huttner, Chem. Ber. 109 (1976) 2033;
(c) P.C. Tang, W.D. Wulff, J. Am. Chem. Soc. 106 (1984) 1132;
(d) M.E. Bos, W.D. Wulff, R.A. Miller, S. Chamberlin, T.A. Brandvold, J. Am. Chem. Soc. 113 (1991) 9293;
(e) M.L. Waters, M.E. Bos, W.D. Wulff, J. Am. Chem. Soc. 121 (1999) 6403;
(f) J. Barluenga, L.A. López, S. Martínez, M. Tomás, Tetrahedron 56 (2000) 4967.

[4] (a) M. Duetsch, R. Lackmann, F. Stein, A. de Meijere, Synlett (1991) 324;
(b) R. Aumann, H. Heinen, M. Dartmann, B. Krebs, Chem. Ber. 124 (1991) 2343;
(c) W.D. Wulff, B.M. Bax, T.A. Brandvold, K.S. Chan, A.M. Gilbert, R.P. Hsung, J. Mitchell, J. Clardy, Organometallics 13 (1994) 102.

[5] (a) F. Stein, M. Duetsch, M. Noltemeyer, A. de Meijere, Synlett (1993) 486;
(b) M. Duetsch, F. Stein, F. Funke, E. Pohl, R. Herbst-Irmer, A. de Meijere, Chem. Ber. 126 (1993) 2535.

[6] (a) F. Funke, M. Duetsh, F. Stein, M. Noltemeyer, A. de Meokere, Chem. Ber. 127 (1994) 911;
(b) R. Aumann, R. Frohlich, F. Zippel, Organometallics 16 (1994) 2571.

[7] Y.T. Wu, B. Flynn, H. Schirmer, F. Funke, S. Muller, T. Labahn, M. Notzel, A. de Meijere, Eur. J. Org. Chem. 4 (2004) 724.

[8] F. Stein, M. Duetsch, R. Lackmann, M. Noltemeyer, A. de Meijere, Angew. Chem. 103 (1991) 1669;
Angew. Chem. Int. Ed. Engl. 30 (1991) 1658.

[9] (a) J. Barluenga, J. Santamaria, M. Tomas, Chem. Rev. 104 (2004) 2259;
(b) A. Muller, A. Maier, R. Neumann, G. Maas, Eur. J. Org. Chem. 6 (1998) 1177;
(c) J. Barluenga, M.A. Fernandez-Rodriguez, E.J. Aguilar, Organomet. Chem. 690 (2005) 539;
(d) J. Barluenga, M. Fananas-Mastral, F. Aznar, Org. Lett. 7 (2005) 1235;
(e) J. Barluenga, Pure Appl. Chem. 74 (2002) 1317.

[10] C.F. Bernasconi, Chem. Soc. Rev. 26 (1997) 299.

[11] (a) C.F. Bernasconi, M. Ali, Organometallics 23 (2004) 6134;
(b) C.F. Bernasconi, S. Bhattacharya, Organometallics 23 (2004) 1722.

[12] A. Arrieta, F.P. Cossío, I. Fermández, M. Gómez-Gallego, B. Lecea, M.J. Mancheño, M.A. Sierra, J. Am. Chem. Soc. 122 (2000) 11509.

[13] M.L. Waters, M.E. Bos, W.D. Wulff, J. Am. Chem. Soc. 121 (1999) 6403.

[14] R. Pipoh, R. van Eldik, G. Henkel, Organometallics 12 (1993) 2236.

[15] R. Pipoh, R. van Eldik, Inorg. Chim. Acta 222 (1994) 207.

[16] R. Pipoh, P. Martinez, R. van Eldik, Ber. Bunsenges. Phys. Chem. 97 (1993) 1435.

[17] R. Pipoh, R. van Eldik, Organometallics 12 (1993) 2668.

[18] K.C. Gu, J.Z. Chen, Z.Y. Zheng, S.Z. Wu, X.W. Wu, X.W. Han, Z.K. Yu, Polyhedron 24 (2005) 173.

[19] P. Govindaswamy, Y.A. Mozharivskyj, M.R. Kollipara, J. Organomet. Chem. 689 (2004) 3265.

[20] R. Aumann, P. Hinterding, Chem. Ber. 126 (1993) 421.

[21] C. Amman, P. Meier, A.E. Merbach, J. Magn. Reson. 46 (1982) 319.

[22] CERIUS 2, Version 4.2, DMOL3, Molecular Simulations Inc., 2000.

[23] L. Joubert, P. Maldivi, J. Phys. Chem. A 105 (2001) 9068.

[24] (a) G. Yang, Y. Wang, D.H. Zhou, J.Q. Zhuang, X.C. Liu, X.W. Han, X.H. Bao, J. Chem. Phys. 119 (2003) 9765;
(b) G. Yang, J.Q. Zhuang, Y. Wang, D.H. Zhou, M.Q. Yang, X.C. Liu, X.W. Han, X.H. Bao, J. Mol. Struct. 737 (2005) 271;
(c) G. Yang, Y. Wang, D.H. Zhou, X.C. Liu, X.W. Han, X.H. Bao, J. Mol. Catal. A 237 (2005) 36.

[25] C.C. Wang, Y. Wang, H.J. Liu, K.J. Lin, L.K. Chou, K.S. Chan, J. Phys. Chem. A 101 (1997) 8887.

[26] F. Aguilar-Parrilla, C. Cativiela, M.D.D. de Villegas, J. Elguero, C. Foces-Foces, J.I.G. Laureiro, F.H. Cano, H.-H. Limbach, J.A.S. Smith, C. Toiron, J. Chem. Soc. Perkin Trans. 2 (10) (1992) 1737.

[27] B.B. Lohray, C.V. Kumar, P.K. Das, M.V. George, J. Org. Chem. 49 (1984) 4647.

[28] S.R. Amin, K.N. Jayaprakash, M. Nandi, K.M. Sathe, A. Sarkar, Organometallics 15 (1996) 3528.

[29] I. Fernández, F.P. Cossío, A. Arrieta, B. Lecea, M.J. Mancheño, M.A. Sierra, Organometallics 23 (2004) 1065.

[30] Following the reaction pathway, structures with N_1 to attack substrate **A** were optimized. However, the reasonable configuration of the first intermediate cannot be reached no matter how we have tried, implying that it would not be N_1 atom that acts as the nucleophilic center. Mulliken population analyses were performed on a series of substituted pyrazoles, showing that charges on N2 atoms (-0.217 to -0.244 |e|) are more negative than that on N1 atoms (-0.125 to -0.155 |e|) in each case (the exact values can be found in Table S2). Accordingly, it is N_2 atom that acts as the nucleophilic center.